Adaptive Filtering with Bandwidth Constraints in the Feedback Path

György Orosz, László Sujbert, Gábor Péceli

Department of Measurement and Information Systems,
Budapest University of Technology and Economics, {orosz, sujbert, peceli}@mit.bme.hu

Abstract

This paper introduces a new, adaptive-filter-based controller that shows advantageous properties from the viewpoint of its communication requirement. The algorithm is called *signed-error filtered-x LMS* (SE-FxLMS). Its novelty is characterized by the fact that it makes possible data compression in the feedback path of adaptive-filter-based control loops in a very simple way. This feature is especially useful in such closed-loop systems where the feedback signals are transmitted over a low-bandwidth communication channel. This is a typical case in so-called networked control systems (NCS) where the communication is carried out over a shared communication channel, e.g., using a wireless sensor network. The paper introduces an analysis of the algorithm as well.

Keywords: wireless control, networked control systems, signed-error algorithm, adaptive filter based controller, FxLMS algorithm

1 Introduction

Recently, so-called networked control systems (NCS) have been attracting the attention of several researchers [1, 2]. The most characteristic property of this kind of system is that the feedback signals are transmitted over a shared communication medium, e.g., Ethernet, Control Area Network (CAN), or wireless networks (ZigBee, Bluetooth, etc.). The advantage of networked communication is that it does not require a point-to-point connection between the units, which decreases the cost of the installation of the system, and the structure can be changed easier than in the case of a fixed connection. The wireless communication further improves the flexibility.

However, networked communication is not accustomed in traditional closed-loop systems, and this raises several issues that have not been considered in conventional algorithm design. The difficulties of networked closed-loop applications originate from the inherent and inevitable problems of networked communication, e.g., bandwidth limit, data loss, and uncertain data transfer time [1,3,4]. The operation of a control loop requires real-time feedback from the sensors, therefore these communication problems have considerable impact on the algorithm design as well.

This paper focuses on the problems of adaptive-filter-based closed-loop systems with a bandwidth-limited communication channel. The issues of bandwidth-limited closed-loop systems have already been investigated by several authors. Most significant results can be found, e.g., in [4,5] and references therein. These papers contain either general results (e.g., minimum data rate theorem) or deal with special control-theoretic algorithms (e.g., LQG control [6]). Adaptive-filter-based algorithms, however, have not been investigated yet in the context of bandwidth-limited closed-loop systems. The novelty of this paper is that it introduces a new, adaptive-filter-based control algorithm that shows advantageous properties from the viewpoint of its bandwidth requirement. This algorithm is a variant of the well-known FxLMS algorithm [7–9], and is called the *signed-error filtered-x least mean square* (SE-FxLMS) algorithm. The SE-FxLMS algorithm achieves bandwidth reduction in the feedback path from the sensors to the central controller with the utilization of the signed-error principle [10], which means that the algorithm uses only the sign of the control error. This method realizes a simple data compression algorithm, and thus decreases the amount of data to be transmitted over the network. The data compression is especially important when the sensor data are transmitted over a low-bandwidth communication channel, or when the system consists of many sensors. The simplicity of the algorithm plays an important role when it is implemented on resource-constrained sensors, which is a typical case for example in wireless sensor networks (WSNs).

The signal compression feature of the signed-error algorithms was experimentally demonstrated in [11], which introduced a wireless active noise control system where a signed-error resonator-based adaptive controller was used for noise control. The signal compression has an important role in this application since it requires real-time transmission of acoustic signals. Unlike the signed-error algorithm introduced in [11], the SE-FxLMS can also be applied in the case of general stochastic reference and control signals, furthermore it preserves the capability of signal compression.

Although signed-error algorithms have already been deployed in various applications, and have been analyzed from several aspects [10,12–17], the analyses in those papers apply to the case when the adaptive algorithm has unfiltered error feedback. In an adaptive noise control system, however, the feedback signal passes through the plant to be controlled, which has a dynamic property characterized by a transfer function. It has already been shown that a dynamic system in the feedback path changes the behavior of adaptive algorithms [18], which makes necessary the analysis of the signed-error FxLMS algorithm as well.

The paper is organized as follows. In Section 2, the SE-FxLMS algorithm is introduced. In Section 3, an upper bound is derived for the mean-absolute error of the algorithm, and the behavior of the adaptive filter's weights is investigated in steady state. Section 4 provides some simulation results that prove the validity of the formulas derived in the paper.

2 Adaptive Algorithm

The FxLMS algorithm [7–9] and its variants are adaptive-filter-based algorithms that strive to minimize the square of the control error by a gradient-based algorithm. A wide-spread application of the FxLMS based algorithms is in the field of active noise and vibration control [19]. These applications involve a large number of free parameters, and FxLMS is capable of controlling systems with complicated transfer functions (e.g., acoustic and complex mechanical systems).

Fig. 1 shows a block diagram of the SE-FxLMS algorithm, where

y'_n : Output signal of the plant, where subscript n is the time index.

y_n : Desired value of the output.

u_n : Control signal, i.e., the input of the plant.

n_n : Noise at the output of the plant.

e_n : Control error: $e_n = y_n - y'_n + n_n$.

x_n : Reference signal, which is assumed to be stationary and ergodic.

$\mathbf{x}_n$: Vector form of x_n formed as $[x_n \ldots x_{n-N+1}]^{\mathrm{T}} \in \mathbb{R}^{N\times 1}$.

$\mathbf{w}_n$: Adaptive filter of length N formed as $\mathbf{w}_n = [w_{0,n} \ \ldots \ w_{N-1,n}]^{\mathrm{T}} \in \mathbb{R}^{N\times 1}$.

$G(z)$: Transfer function of the stable, linear plant, which is characterized by its impulse response g_n.

$\hat{G}(z)$: Estimate of the plant. In this paper we do not deal with modeling errors in the plant, so $\hat{G}(z) = G(z)$.

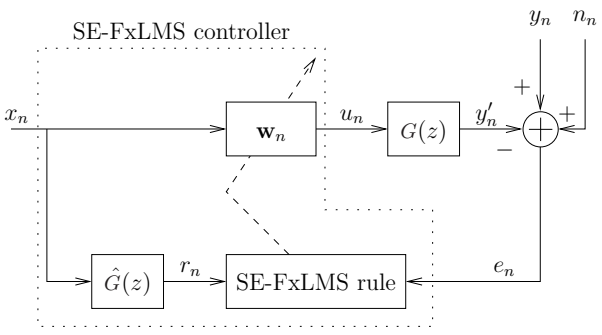

Figure 1: Block diagram of the signed-error FxLMS algorithm

The adaptive algorithm decreases the error by continuously updating the filter coefficients ($\mathbf{w}_n$) using a gradient-based method. The control signal u_n is generated from the reference signal x_n, so x_n and y_n are correlated.

The essential difference between the "conventional" and signed-error adaptive algorithms is that while the former uses the full error signal in the parameter updating, the latter uses only the sign of the error signal. Since the FxLMS parameter updating is: $\mathbf{w}_{n+1} = \mathbf{w}_n + \mu \mathbf{r}_n e_n$ [7,9], the parameter updating rule of the SE-FxLMS algorithm is:

$$\mathbf{w}_{n+1} = \mathbf{w}_n + \mu \mathbf{r}_n \operatorname{sign}(e_n), \tag{1}$$

where μ is a positive convergence parameter, $\operatorname{sign}(\cdot)$ stands for the sign function[1] , and $\mathbf{r}_n = [r_n \dots r_{n-N+1}]^{\mathrm{T}} \in \mathbb{R}^{N\times 1}$ is the filtered reference signal vector:

$$r_n = \sum_{k=0}^{\infty} g_k x_{n-k} \leftrightarrow \mathbf{r}_n = \sum_{k=0}^{\infty} g_k \mathbf{x}_{n-k}, \tag{2}$$

where we assume a perfect plant estimate $\hat{g}_k = g_k$, which is the impulse response of $G(z)$.

The control signal is obtained by filtering the reference signal with the adaptive filter:

$$u_n = \sum_{i=0}^{N-1} w_{i,n} x_{n-i} = \mathbf{x}_n^{\mathrm{T}} \mathbf{w}_n. \tag{3}$$

The step-by-step description of the SE-FxLMS algorithm

loop

Calculate the control signal u_n from (3), and apply it to the plant.

Calculate the filtered reference $\mathbf{r}_n$: (2).

Read the error signal from the sensor, and update the filter $\mathbf{w}_n$: (1).

end loop

As it can be noted, the SE-FxLMS updating rule uses only the sign of the error signal, which makes the computation simpler since multiplication by a sign function only involves manipulation of the sign of the multiplicand.

The main advantage of the SE-FxLMS algorithm is that it offers a very simple method for data compression. Since the signal compression truncates the error, the algorithm is easy to implement in systems with limited resources, e.g., in wireless sensor networks. The drawback of the algorithm is that the truncation of the error results generally in longer convergence and higher steady-state error compared to the FxLMS.

The signal compressing feature of the algorithm is especially important in closed-loop systems where a central signal processing unit (that implements the adaptive algorithm) and the sensor are separated, and are connected over a low-bandwidth communication channel. This is a very common case in networked control systems [4, 5]. A simplified block diagram of such a system is shown in Fig. 2. If the sensor transmits only the sign of the error signal, significant reduction in the amount of data can be achieved. In practical applications, the case $\operatorname{sign}(e_n) = 0$ usually has marginal significance, so $\operatorname{sign}(e_n)$ can be represented by one bit that indicates whether e_n is positive or negative (+/–). This means that assuming b bit resolution of the error signal, the data to be transmitted over the network can be reduced to $1/b$ of the original amount of data. Thus, a significant reduction is achieved even if the communication overhead is taken into account. An experimental illustration of the signal compressing feature of the signed-error algorithms can be found in [11] within the frame of a wireless active noise control system.

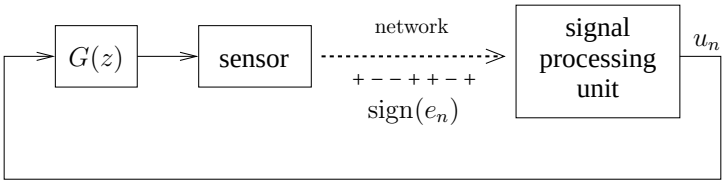

Figure 2: Networked closed-loop system equipped with the signed-error algorithm

[1] $\operatorname{sign}(x) = +1$ if $x > 0$; $\operatorname{sign}(x) = -1$ if $x < 0$; $\operatorname{sign}(x) = 0$ if $x = 0$

3 Analysis

As (1) shows, the vector $\mathbf{w}_n$ is updated irrespectively of the magnitude of the error signal, even in the tight optimal region where the error is small. This causes fluctuation of the parameter values around the optimum so the error signal cannot be set to zero even in the optimal case. This residual error is one of the most commonly investigated properties of the signed-error algorithms [13], and is generally characterized by the mean-absolute error (MAE), which will be derived for the SE-FxLMS in this section.

The model of the impulse response g_k, associated with $G(z)$, can be made more realistic if it is assumed that it includes at least d samples of delay. This is especially true for NCSs where the communication network introduces transport delay, which is prepended to the impulse response of the physical plant. This statement is formalized as:

$$\gamma_k = g_{k+d}, \tag{4}$$

where $g_k = 0$ for $k < d$, and γ_k denotes the part of the impulse response that does not include any delay. The impulse response g_k should be identified before starting the operation of the algorithm, and γ_k can be extracted from g_k by removing the leading zero elements. Fig. 5 shows a real identification example where the delay and γ_k are clearly distinguishable.

It is shown in Appendix A that y'_n can be calculated as follows:

$$y'_n = \mathbf{r}_n^{\mathrm{T}}\mathbf{w}_{n'} - h_n \ , \quad n' = n - d, \tag{5}$$

where

$$h_n = \mu \sum_{k=1}^{\infty}\sum_{q=1}^{k} \gamma_k \mathbf{x}_{n'-k}^{\mathrm{T}}\mathbf{r}_{n'-q}\,\mathrm{sign}(e_{n'-q}). \tag{6}$$

The desired value of the plant output can be modeled as follows [9]:

$$y_n = \mathbf{r}_n^{\mathrm{T}}\mathbf{w}_{\mathrm{o}}, \tag{7}$$

where $\mathbf{w}_{\mathrm{o}}$ denotes the optimal parameter vector. In the ideal and noiseless case, this signal can be completely tracked by the algorithm, so that if $\mathbf{w}_n \equiv \mathbf{w}_{\mathrm{o}}$ were fixed, the error would become zero, and $y'_n \equiv y_n$ since $h_n = 0$ if the error is zero—see (6). External disturbances and modeling error can be represented by an additional noise term n_n [9]. Modeling error refers to how precisely reality is described by (7), and can be reduced by increasing N.

The error signal can be expressed from (5) and (7):

$$e_n = y_n - y'_n + n_n = \mathbf{r}_n^{\mathrm{T}}(\mathbf{w}_{\mathrm{o}} - \mathbf{w}_{n'}) + h_n + n_n. \tag{8}$$

One can define the error of the parameter vector:

$$\tilde{\mathbf{w}}_n = \mathbf{w}_n - \mathbf{w}_{\mathrm{o}}. \tag{9}$$

So (8) can be rewritten:

$$\begin{aligned} e_n &= \mathbf{r}_n^{\mathrm{T}}(\mathbf{w}_{\mathrm{o}} - \mathbf{w}_n + \mathbf{w}_n - \mathbf{w}_{n'}) + h_n + n_n \\ &= -\mathbf{r}_n^{\mathrm{T}}\tilde{\mathbf{w}}_n + \mathbf{r}_n^{\mathrm{T}}(\mathbf{w}_n - \mathbf{w}_{n'}) + h_n + n_n. \end{aligned} \tag{10}$$

The updating rule can also be defined for $\tilde{\mathbf{w}}_n$ according to (1) and (9):

$$\tilde{\mathbf{w}}_{n+1} = \tilde{\mathbf{w}}_n + \mu\mathbf{r}_n\,\mathrm{sign}(e_n). \tag{11}$$

3.1 Calculation of Mean-Absolute Error

In this subsection, an explicit formula of the MAE is derived, and it is shown to be proportional to the convergence parameter μ.

Let's multiply $\tilde{\mathbf{w}}_{n+1}$ in (11) by its transpose, which provides the squared Eucledian norm, and using the fact that $\mathbf{r}_n^{\mathrm{T}}\tilde{\mathbf{w}}_n = \tilde{\mathbf{w}}_n^{\mathrm{T}}\mathbf{r}_n$ one obtains:

$$\begin{aligned} \|\tilde{\mathbf{w}}_{n+1}\|^2 = \tilde{\mathbf{w}}_{n+1}^{\mathrm{T}}\tilde{\mathbf{w}}_{n+1} &= \left[\tilde{\mathbf{w}}_n + \mu\mathbf{r}_n\,\mathrm{sign}(e_n)\right]^{\mathrm{T}}\left[\tilde{\mathbf{w}}_n + \mu\mathbf{r}_n\,\mathrm{sign}(e_n)\right] \\ &= \|\tilde{\mathbf{w}}_n\|^2 + \mu^2\,\mathrm{sign}(e_n)\mathbf{r}_n^{\mathrm{T}}\mathbf{r}_n\,\mathrm{sign}(e_n) + 2\mu\,\mathrm{sign}(e_n)\mathbf{r}_n^{\mathrm{T}}\tilde{\mathbf{w}}_n. \end{aligned} \tag{12}$$

Solving (10) for $\mathbf{r}_n^{\mathrm{T}}\tilde{\mathbf{w}}_n$, substituting into (12), and taking the expectation of both sides yields:

$$\begin{aligned}\mathbb{E}\left\{\|\tilde{\mathbf{w}}_{n+1}\|^2\right\} &= \mathbb{E}\left\{\|\tilde{\mathbf{w}}_n\|^2\right\} + \mu^2\mathbb{E}\left\{\operatorname{sign}(e_n)\mathbf{r}_n^{\mathrm{T}}\mathbf{r}_n\operatorname{sign}(e_n)\right\}\\ &+ 2\mu\mathbb{E}\left\{\operatorname{sign}(e_n)\mathbf{r}_n^{\mathrm{T}}(\mathbf{w}_n-\mathbf{w}_{n'})\right\} + 2\mu\mathbb{E}\left\{\operatorname{sign}(e_n)h_n\right\}\\ &+ 2\mu\mathbb{E}\left\{\operatorname{sign}(e_n)n_n\right\} - 2\mu\mathbb{E}\left\{\operatorname{sign}(e_n)e_n\right\}. \end{aligned} \tag{13}$$

In (13), $\operatorname{sign}(e_n)e_n = |e_n|$, and furthermore, $\operatorname{sign}(e_n)n_n \le |n_n|$, $\operatorname{sign}(e_n)h_n \le |h_n|$, $\operatorname{sign}(e_n)\mathbf{r}_n^{\mathrm{T}}\mathbf{r}_n\operatorname{sign}(e_n) \le |\mathbf{r}_n^{\mathrm{T}}\mathbf{r}_n|$, and $\operatorname{sign}(e_n)\mathbf{r}_n^{\mathrm{T}}(\mathbf{w}_n-\mathbf{w}_{n'}) \le |\mathbf{r}_n^{\mathrm{T}}(\mathbf{w}_n-\mathbf{w}_{n'})|$ since $\operatorname{sign}(e_n)\in\{+1,0,-1\}$. Hence (13) can be rewritten:

$$\begin{aligned}\mathbb{E}\left\{\|\tilde{\mathbf{w}}_{n+1}\|^2\right\} &\le \mathbb{E}\left\{\|\tilde{\mathbf{w}}_n\|^2\right\} + \mu^2\mathbb{E}\left\{|\mathbf{r}_n^{\mathrm{T}}\mathbf{r}_n|\right\}\\ &+ 2\mu\mathbb{E}\left\{|\mathbf{r}_n^{\mathrm{T}}(\mathbf{w}_n-\mathbf{w}_{n'})|\right\} + 2\mu\mathbb{E}\left\{|h_n|\right\}\\ &+ 2\mu\mathbb{E}\left\{|n_n|\right\} - 2\mu\mathbb{E}\left\{|e_n|\right\}. \end{aligned} \tag{14}$$

Upper bounds of the scalar components of (14) are derived in Appendix B, so using (B-8), (B-4) and (B-5) in (14) yields:

$$\begin{aligned}\mathbb{E}\left\{\|\tilde{\mathbf{w}}_{n+1}\|^2\right\} &\le \mathbb{E}\left\{\|\tilde{\mathbf{w}}_n\|^2\right\} + \mu^2 N\rho_{\mathrm{w}}\\ &+2\mu^2 N\rho_{\mathrm{d}} + 2\mu^2 N\rho_{\mathrm{p}} + 2\mu\varepsilon - 2\mu\mathbb{E}\left\{|e_n|\right\}, \end{aligned} \tag{15}$$

where

$$\varepsilon \triangleq \mathbb{E}\left\{|n_n|\right\} \tag{16}$$

is the absolute-mean value of the noise, and

$$\rho_{\mathrm{w}} = R_{|r|\,|r|}(0), \tag{17a}$$

$$\rho_{\mathrm{d}} = \sum_{q=1}^{d} R_{|r|\,|r|}(q), \tag{17b}$$

$$\rho_{\mathrm{p}} = \sum_{k=1}^{\infty}\sum_{q=1}^{k} |\gamma_k| R_{|x|\,|r|}(k-q). \tag{17c}$$

where $R_{|r|\,|r|}(\tau)\triangleq\mathbb{E}\left\{|r_t|\cdot|r_{t+\tau}|\right\}$ denotes the correlation function, and it is assumed that x_n, r_n, and n_n are stationary processes. Iterating (15) backward with $(n-1)$ steps and dividing both sides by 2μ yields:

$$\begin{aligned}\frac{1}{2\mu}\mathbb{E}\left\{\|\tilde{\mathbf{w}}_{n+1}\|^2\right\} &\le \frac{1}{2\mu}\mathbb{E}\left\{\|\tilde{\mathbf{w}}_1\|^2\right\} + n\frac{1}{2}\mu N\rho_{\mathrm{w}}\\ &+n\mu N\rho_{\mathrm{d}} + n\mu N\rho_{\mathrm{p}} + n\varepsilon - \sum_{i=1}^{n}\mathbb{E}\left\{|e_i|\right\}. \end{aligned} \tag{18}$$

Since $\mathbb{E}\left\{\|\tilde{\mathbf{w}}_{n+1}\|^2\right\} \ge 0$, rearranging (18), and dividing both sides by n gives the MAE:

$$\begin{aligned}E^{\mathrm{a}} = \frac{1}{n}\sum_{i=1}^{n}\mathbb{E}\left\{|e_i|\right\} &\le \frac{1}{2n\mu}\mathbb{E}\left\{\|\tilde{\mathbf{w}}_1\|^2\right\}\\ &+\mu N\left(\frac{1}{2}\rho_{\mathrm{w}} + \rho_{\mathrm{d}} + \rho_{\mathrm{p}}\right) + \varepsilon. \end{aligned} \tag{19}$$

The estimation of the MAE is used in most cases to characterize the steady-state MAE ($E_{\mathrm{ss}}^{\mathrm{a}}$) of the signed-error algorithms, i.e., one can calculate an upper bound of the MAE that can be guaranteed. Let $\bar{E}_{\mathrm{ss}}^{\mathrm{a}}$ denote an upper bound on the steady-state error. To calculate $\bar{E}_{\mathrm{ss}}^{\mathrm{a}}$, (19) should be used with $n\to\infty$, which results in:

$$E_{\mathrm{ss}}^{\mathrm{a}} = \lim_{n\to\infty}\frac{1}{n}\sum_{i=1}^{n}\mathbb{E}\left\{|e_i|\right\} \le \mu N\left(\frac{1}{2}\rho_{\mathrm{w}} + \rho_{\mathrm{d}} + \rho_{\mathrm{p}}\right) + \varepsilon = \bar{E}_{\mathrm{ss}}^{\mathrm{a}}, \tag{20}$$

where ρ_{w}, ρ_{d}, ρ_{p}, and ε are determined by the reference signal, the plant $G(z)$, and the noise process, so these parameters are physically constrained.

In (20), two design parameters are found: N and μ. Here, N is the length of the adaptive filter, which should be long enough so that it can track the desired signal y_n described by (7). The value of N is often chosen experimentally or using physical considerations. The other design parameter, μ, is used to set the steady-state error and the transient response. If an upper bound of the steady-state MAE, $\bar{E}^{\mathrm{a}}_{\mathrm{ss}}$, is given, rearranging (20) gives

$$\mu = \frac{\bar{E}^{\mathrm{a}}_{\mathrm{ss}} - \varepsilon}{N\left(\frac{1}{2}\rho_{\mathrm{w}} + \rho_{\mathrm{d}} + \rho_{\mathrm{p}}\right)}. \tag{21}$$

3.2 Discussion

The terms in (19) can be divided into three groups according to their effect on the MAE. The last term in (19), ε, is the mean-absolute value of the noise, which cannot be controlled by the convergence parameter, and sets a lower limit on the MAE.

The first term, $\frac{1}{2n\mu}\mathbb{E}\left\{\|\tilde{\mathbf{w}}_1\|^2\right\}$, can be associated with the transient error since in steady state, as $n \to \infty$, it tends to zero. Since this term is proportional to $\frac{1}{\mu}$, the smaller the parameter μ is, the longer the transient lasts. However, (19) is generally used for estimating the steady-state MAE when $\frac{1}{2n\mu}\mathbb{E}\left\{\|\tilde{\mathbf{w}}_1\|^2\right\} \to 0$, because $\tilde{\mathbf{w}}_1$ (the initial parameter error) is unknown in most cases since that would require knowledge of the optimal solution.

In (19), $\mu N\left(\frac{1}{2}\rho_{\mathrm{w}} + \rho_{\mathrm{d}} + \rho_{\mathrm{p}}\right)$ is the part of the MAE that results from the constant weight update, i.e., the parameters are changed using the sign of the error, irrespectively of its magnitude. As (19) shows, the steady-state MAE can be set with μ (apart from the noise floor), so it is an important design parameter. Small steady-state error requires small μ, which in turn results in a longer transient since the parameters are modified at each update with small steps. Note that the upper bound on the steady-state MAE given by (20) is linearly proportional to μ, hence any finite value of μ assures the stability of the algorithm in the sense that steady-state MAE remains bounded. These important features are also observable in the case of the simple signed-error LMS algorithm [10].

Comparing the MAE of the SE-FxLMS with that of the basic signed-error LMS algorithm [10], the essential difference is that the presence of a dynamic system between the output and input of the algorithm causes an increase in the MAE. This growth is represented by $(\rho_{\mathrm{p}} + \rho_{\mathrm{d}})$ in the MAE (19).

The question may arise as to why is it important to separate the delay from the impulse response in the calculation of E^{a}. Actually, it is not necessary to make this separation since it is not required in the proof that γ_k does not include any delay. Therefore it is allowable to use $d = 0$ and g_k instead of γ_k, however, numerical calculations for several plants and parameter settings show that this kind of separation of the delay yields a tighter bound on the MAE. This property is important in the design phase since the convergence parameter μ is often chosen according to the desired MAE: if the upper bound of the MAE is given, then μ can be calculated according to (21). So, if a tighter bound on MAE is found, then higher μ can be used, which results in faster convergence.

3.3 Filter Weight Behavior in Steady State

In this subsection, it is shown that in the case of a Gaussian reference signal, the optimal parameter vector, $\mathbf{w}_{\mathrm{o}}$, is the Wiener solution, and the expected distance of the filter weights from the optimum is bounded in steady state.

The optimal solution of the SE-FxLMS can be traced back to the SE-LMS algorithm. The reason is that if the filter $\mathbf{w}_n$ is set permanently to the optimal solution, i.e., $\mathbf{w}_n \equiv \mathbf{w}_{\mathrm{o}}$, the blocks $\mathbf{w}_n$ and $G(z)$ in Fig. 1 are interchangeable since they are linear time-invariant systems. This results in a structure equivalent to that of the SE-LSM whose reference input signal is r_n. This structure has already been investigated in [10], where it is shown that the optimal solution is unique if the autocorrelation matrix of r_n is positive definite. This condition is the same as in the case of the LMS algorithm, however, the essential difference is that signed-error algorithms minimize the mean-absolute error, $\mathbb{E}\{|e_n|\}$, since $\frac{d|e_n|}{de_n} = \mathrm{sign}(e_n)$. Generally it results in a different optimal solution than that of the LMS algorithm [10], however, for Gaussian reference signal, the Wiener solution [7] also minimizes the cost function $\mathbb{E}\{|e_n|\}$, as well as $\mathbb{E}\left\{e_n^2\right\}$ [20].

The parameter error, i.e., the distance of the filter coefficients from the optimum, can be characterized by the mean-square parameter error norm, $\mathbb{E}\left\{\|\tilde{\mathbf{w}}_n\|^2\right\}$. We perform the analysis for ergodic and Gaussian x_n and e_n, which allows us to use the following equality for any Gaussian signal, ξ, [16]:

$$\mathbb{E}\left\{\xi^2\right\} = \frac{\pi}{2}\mathbb{E}\left\{|\xi|\right\}^2. \tag{22}$$

It is also assumed that the autocorrelation matrix of the filtered reference signal is positive definite. Furthermore, we use the simplifying notation:

$$h'_n = \mathbf{r}_n^{\mathrm{T}}(\mathbf{w}_n - \mathbf{w}_{n'}) + h_n, \tag{23}$$

so $\mathbf{r}_n^{\mathrm{T}}\tilde{\mathbf{w}}_n = h'_n + n_n - e_n$ according to (10). Left multiplying $\mathbf{r}_n^{\mathrm{T}}\tilde{\mathbf{w}}_n$ by its transpose and taking the expectation gives:

$$\begin{aligned}
&\mathbb{E}\left\{\tilde{\mathbf{w}}_n^{\mathrm{T}}\mathbf{r}_n\mathbf{r}_n^{\mathrm{T}}\tilde{\mathbf{w}}_n\right\} = \\
&= \mathbb{E}\left\{h_n'^2\right\} + \mathbb{E}\left\{n_n^2\right\} + \mathbb{E}\left\{e_n^2\right\} - 2\mathbb{E}\left\{e_n n_n\right\} - 2\mathbb{E}\left\{e_n h'_n\right\} + 2\mathbb{E}\left\{h'_n n_n\right\} \\
&\leq \mathbb{E}\left\{h_n'^2\right\} + \mathbb{E}\left\{n_n^2\right\} + \mathbb{E}\left\{e_n^2\right\} + 2\sqrt{\mathbb{E}\left\{e_n^2\right\}\mathbb{E}\left\{n_n^2\right\}} + 2\sqrt{\mathbb{E}\left\{e_n^2\right\}\mathbb{E}\left\{h_n'^2\right\}} \\
&= \mathbb{E}\left\{h_n'^2\right\} + \mathbb{E}\left\{n_n^2\right\} + \mathbb{E}\left\{e_n^2\right\} + 2\sqrt{\mathbb{E}\left\{e_n^2\right\}}\left(\sqrt{\mathbb{E}\left\{h_n'^2\right\}} + \sqrt{\mathbb{E}\left\{n_n^2\right\}}\right)
\end{aligned} \tag{24}$$

where we have used the Cauchy-Schwarz inequality[2]. Furthermore h'_n and n_n are treated as independent, since h'_n contains noise-dependent components only for time indices $i < n$. Hence $\mathbb{E}\{h'_n n_n\} = \mathbb{E}\{h'_n\}\mathbb{E}\{n_n\} = \mathbb{E}\{h'_n\}\cdot 0$. To calculate an upper bound for the expected value of the squared terms, we use (22), (23), (B-5), (B-8), and (16):

$$\mathbb{E}\left\{h_n'^2\right\} + \mathbb{E}\left\{n_n^2\right\} \leq \tfrac{\pi}{2}\mu^2 N^2\left(\rho_{\mathrm{d}} + \rho_{\mathrm{p}}\right)^2 + \tfrac{\pi}{2}\varepsilon^2, \tag{25}$$

$$2(\sqrt{\mathbb{E}\left\{h_n'^2\right\}} + \sqrt{\mathbb{E}\left\{n_n^2\right\}}) \leq 2\left[\sqrt{\tfrac{\pi}{2}}\mu N\left(\rho_{\mathrm{d}} + \rho_{\mathrm{p}}\right) + \sqrt{\tfrac{\pi}{2}}\varepsilon\right], \tag{26}$$

$$\mathbb{E}\left\{e_n^2\right\} = \tfrac{\pi}{2}\mathbb{E}\left\{|e_n|\right\}^2 \leq \tfrac{\pi}{2}(\bar{E}_{\mathrm{ss}}^{\mathrm{a}})^2. \tag{27}$$

In (27), $\mathbb{E}\{|e_n|\}$ has been obtained from (20) for steady state:

$$\bar{E}_{\mathrm{ss}}^{\mathrm{a}} \geq \lim_{k\to\infty}\frac{1}{k}\sum_{n=1}^{k}\mathbb{E}\left\{|e_n|\right\} = \mathbb{E}\left\{\lim_{k\to\infty}\frac{1}{k}\sum_{n=1}^{k}|e_n|\right\} = \mathbb{E}\left\{\mathbb{E}\left\{|e_n|\right\}\right\} = \mathbb{E}\left\{|e_n|\right\}, \tag{28}$$

where we have used the fact that $\lim_{k\to\infty}\frac{1}{k}\sum_{n=1}^{k}\xi_n$ yields the expected value, $\mathbb{E}\{\xi_n\}$, for ergodic signals.

Now we invoke the independence assumption that is often used in papers dealing with the analysis of adaptive algorithms, e.g., [7, 14, 16]. This assumption is reasonable for $\mu \to 0$ [7], however, theoretical results agree generally well with practice without this constraint as well. The independence assumption states that $\tilde{\mathbf{w}}_n$ and $\mathbf{r}_n$ are statistically independent, so:

$$\begin{aligned}
&\mathbb{E}\left\{\tilde{\mathbf{w}}_n^{\mathrm{T}}\mathbf{r}_n\mathbf{r}_n^{\mathrm{T}}\tilde{\mathbf{w}}_n\right\} = \mathbb{E}\left\{\tilde{\mathbf{w}}_n^{\mathrm{T}}\mathbb{E}\left\{\mathbf{r}_n\mathbf{r}_n^{\mathrm{T}}|\tilde{\mathbf{w}}_n\right\}\tilde{\mathbf{w}}_n\right\} = \\
&= \mathbb{E}\left\{\tilde{\mathbf{w}}_n^{\mathrm{T}}\mathbb{E}\left\{\mathbf{r}_n\mathbf{r}_n^{\mathrm{T}}\right\}\tilde{\mathbf{w}}_n\right\} = \mathbb{E}\left\{\tilde{\mathbf{w}}_n^{\mathrm{T}}\mathbf{R}_{rr}\tilde{\mathbf{w}}_n\right\} \geq \lambda_1\mathbb{E}\left\{\left\|\tilde{\mathbf{w}}_n\right\|^2\right\}
\end{aligned} \tag{29}$$

where $\mathbb{E}\{\cdot|\tilde{\mathbf{w}}_n\}$ stands for conditional expectation, and $\mathbf{R}_{rr}$ denotes the autocorrelation matrix of $\mathbf{r}_n$ with eigenvalues $0 < \lambda_1 \leq \ldots \leq \lambda_N$. To obtain $\mathbb{E}\left\{\left\|\tilde{\mathbf{w}}_n\right\|^2\right\}$, (25), (26), (27), and (29) can be substituted into (24):

$$\begin{aligned}
\mathbb{E}\left\{\left\|\tilde{\mathbf{w}}_n\right\|^2\right\} \leq \frac{\pi}{2\lambda_1}\{&\mu^2 N^2\left(\rho_{\mathrm{d}} + \rho_{\mathrm{p}}\right)^2 + \varepsilon^2 + \\
&(\bar{E}_{\mathrm{ss}}^{\mathrm{a}})^2 + 2\left[\mu N\left(\rho_{\mathrm{d}} + \rho_{\mathrm{p}}\right) + \varepsilon\right]\bar{E}_{\mathrm{ss}}^{\mathrm{a}}\},
\end{aligned} \tag{30}$$

where $\bar{E}_{\mathrm{ss}}^{\mathrm{a}}$ is defined in (20). The main conclusion is that the least upper bound on $\mathbb{E}\left\{\left\|\tilde{\mathbf{w}}_n\right\|^2\right\}$ is primarily limited by the noise term, ε, which is a physical constraint. $\mathbb{E}\left\{\left\|\tilde{\mathbf{w}}_n\right\|^2\right\}$ can be set arbitrarily close to this theoretical limit by decreasing μ. In the noiseless case, $\mathbb{E}\left\{\left\|\tilde{\mathbf{w}}_n\right\|^2\right\} \to 0$ if $\mu \to 0$, i.e., the filter parameters can be forced arbitrarily close to the optimal solution. It is also important that, unlike in the case of FxLMS, the norm of the parameter error remains bounded for any μ.

[2] for random variables a and b: $\mathbb{E}\{ab\} \leq \sqrt{\mathbb{E}\{a^2\}\mathbb{E}\{b^2\}}$

3.4 Calculation of the Correlation Functions

This subsection provides a guide as to how the parameters ρ_{w}, ρ_{d}, and ρ_{p} can be calculated according to (17). The difficulty is that the calculation of these parameters requires knowledge of the correlation functions $R_{|r|\,|r|}(q)$ and $R_{|x|\,|r|}(q)$, which are nonlinear functions of the reference and filtered-reference signals x and r, respectively.

Two methods will be shown for calculating the correlation functions. The first one is a numerical calculation according to (B-1) as follows:

1. Generate a signal sequence x_k of length M, which can be generated according to some *a priori* knowledges (e.g., distribution, variance). The value of M should be large enough to calculate the correlation with sufficient accuracy.
2. Generate the filtered reference signal r_k: $r_k = x_k \star g_k$—see (2).
3. Take the absolute value of the sequences x_k and r_k.
4. The correlation functions can be estimated by numerically evaluating (B-1) as follows [21]:

$$R_{|r|\,|r|}(q) \approx \frac{1}{M-|q|}\sum_{i=0}^{M-1}|r_i|\cdot|r_{i+q}|$$
$$R_{|x|\,|r|}(q) \approx \frac{1}{M-|q|}\sum_{i=0}^{M-1}|x_i|\cdot|r_{i+q}|. \tag{31}$$

The correlation functions can also be calculated analytically in some special cases. Let z and w be general stochastic signals with Gaussian distribution. If $R_{zw}(\tau)$, i.e., the cross-correlation of z and w is known, $R_{|z|\,|w|}(\tau)$ can be calculated according to the results in [22, 23]:

$$R_{|z|\,|w|}(\tau) = \alpha\big[R_{zw}(\tau), \sigma_{zw}\big], \tag{32}$$

where

$$\sigma_{zw} = \sqrt{R_{z,z}(0)R_{w,w}(0)} \tag{33}$$

and

$$\alpha[\rho(\tau),\sigma] = \frac{2\sigma}{\pi}\left[\frac{\rho(\tau)}{\sigma}\operatorname{asin}\left(\frac{\rho(\tau)}{\sigma}\right)+\sqrt{1-\left(\frac{\rho(\tau)}{\sigma}\right)^2}\right]. \tag{34}$$

Furthermore:

$$R_{xr}(q) = R_{xx}(q)\star g_q, \tag{35}$$
$$R_{rr}(q) = R_{xx}(q)\star g_q \star g_{-q}, \tag{36}$$

where $\star$ denotes the convolution operator. It is assumed that $R_{xx}(q)$, i.e., the autocorrelation function of x, is available for the calculations. Hence:

$$R_{|x|\,|r|}(q) = \alpha\big[R_{xr}(q), \sigma_{xr}\big], \tag{37}$$
$$R_{|r|\,|r|}(q) = \alpha\big[R_{rr}(q), \sigma_{rr}\big]. \tag{38}$$

4 Simulation Results

This section presents simulations that reflect the most important properties of the SE-FxLMS. We also investigate how the steady-state MAE ($\mathrm{MAE_{ss}}$) can be predicted by the upper bound given in (20).

In all the simulations: $N = 10$, $\varepsilon = 0$, and the reference signal, x_n, is a white Gaussian random process with variance $R_{xx}(0) = 1$, unless otherwise noted.

First, we demonstrate how the non-unity feedback affects the MAE of the signed-error algorithms. Fig. 3 shows a simulation with the SE-FxLMS where $G(z) = z^{-50}$, i.e., a 50-sample delay, and the step size is: $\mu = 5\cdot 10^{-3}$. The $\mathrm{MAE_{ss}}$ obtained from the simulation is 0.13. An upper bound on the $\mathrm{MAE_{ss}}$ calculated using the results for the simple SE-LMS is $\mu N R_{xx}(0)/2 = 0.025$ [10], which gives an incorrect bound for the SE-FxLMS algorithm. However, the upper bound given by (20) yields: $\bar{E}^{\mathrm{a}}_{\mathrm{ss}} = 1.62$.

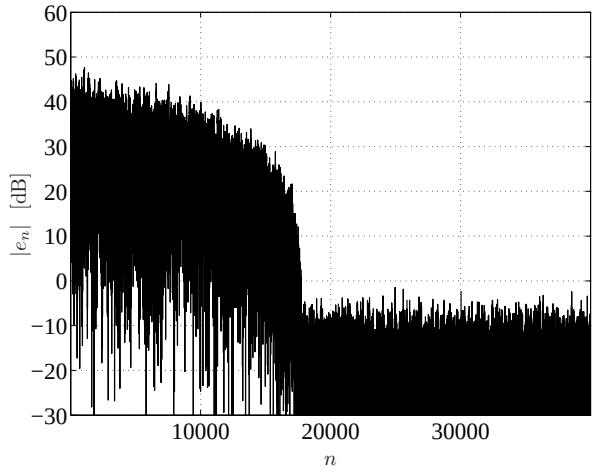

Figure 3: Convergence of the SE-FxLMS with simple delayed feedback: $G(z) = z^{-50}$.

This upper bound is not tight, nevertheless it is a valid result. This experiment shows that even a simple delayed feedback causes an increase of $\mathrm{MAE}_{\mathrm{ss}}$, which cannot be handled by existing results regarding signed-error adaptive filters.

The SE-FxLMS algorithm has also been tested with a more complicated $G(\mathrm{z})$, and has been compared to the FxLMS algorithm as well. Here, we present results for a second-order IIR system with $d = 20$:

$$G(z) = 2\frac{z^2 + 0.6627z + 0.6214}{z^2 - 0.3373z + 0.81}z^{-d}. \tag{39}$$

In Fig. 4, the convergence of the SE-FxLMS (gray) and FxLMS (black) algorithms can be seen. The step sizes are: $\mu = 10^{-3}$ for the SE-FxLMS and $\mu = 10^{-4}$ for the FxLMS. Comparing the convergence of the algorithms, one can observe that, unlike the FxLMS, which ensures exponentially-decreasing error, the MAE of the SE-FxLMS does not decrease below a certain level. The degradation of the residual error compared to FxLMS is the result of the fact that the magnitude of the error is neglected during the adaptation, i.e., only the sign of the error is used.

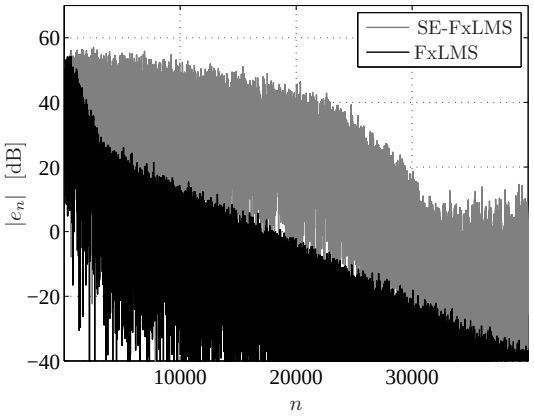

Figure 4: Convergence of the SE-FxLMS (gray) and the FxLMS (black) algorithms

Table 1 summarizes the results of simulations, showing how the parameters μ, N, ε, and d influence the $\mathrm{MAE}_{\mathrm{ss}}$. Each block of the table corresponds to the change of one parameter, while the other parameters are set to the following default values: $\mu = 10^{-3}$, $N = 10$, $\varepsilon = 0$, and $d = 20$. The first row of each block indicates the investigated parameter and its values used in the simulations. In the first column, $E^{\mathrm{a}}_{(\mathrm{S})}$ denotes the $\mathrm{MAE}_{\mathrm{ss}}$ value that is obtained from the simulations. The values $\bar{E}^{\mathrm{a}}_{\mathrm{ss}}$ and $\bar{E}^{\mathrm{a}+}_{\mathrm{ss}}$ denote the

$\mathrm{MAE_{ss}}$ bounds computed using (20), however, $\bar{E}^{\mathrm{a}+}_{\mathrm{ss}}$ was calculated without separating the delay from the dynamic part of $G(z)$.

Table 1: The effect of μ, N, delay and noise on $\mathrm{MAE_{ss}}$; reference signal: white Gaussian process

μ	$1.00 \cdot 10^{-3}$	$1.00 \cdot 10^{-2}$	$1.00 \cdot 10^{-1}$	$1.00 \cdot 10^{0}$
$E^{\mathrm{a}}_{(\mathrm{S})}$	$6.32 \cdot 10^{-1}$	$5.91 \cdot 10^{0}$	$6.08 \cdot 10^{1}$	$5.93 \cdot 10^{2}$
$\bar{E}^{\mathrm{a}}_{\mathrm{ss}}$	$5.43 \cdot 10^{0}$	$5.43 \cdot 10^{1}$	$5.43 \cdot 10^{2}$	$5.43 \cdot 10^{3}$
$\bar{E}^{\mathrm{a}+}_{\mathrm{ss}}$	$1.11 \cdot 10^{1}$	$1.11 \cdot 10^{2}$	$1.11 \cdot 10^{3}$	$1.11 \cdot 10^{4}$
N	5	10	20	50
$E^{\mathrm{a}}_{(\mathrm{S})}$	$3.48 \cdot 10^{-1}$	$6.32 \cdot 10^{-1}$	$1.42 \cdot 10^{0}$	$2.62 \cdot 10^{0}$
$\bar{E}^{\mathrm{a}}_{\mathrm{ss}}$	$2.71 \cdot 10^{0}$	$5.43 \cdot 10^{0}$	$1.09 \cdot 10^{1}$	$2.71 \cdot 10^{1}$
$\bar{E}^{\mathrm{a}+}_{\mathrm{ss}}$	$5.56 \cdot 10^{0}$	$1.11 \cdot 10^{1}$	$2.22 \cdot 10^{1}$	$5.56 \cdot 10^{1}$
d	1	10	20	50
$E^{\mathrm{a}}_{(\mathrm{S})}$	$2.93 \cdot 10^{-1}$	$4.64 \cdot 10^{-1}$	$6.32 \cdot 10^{-1}$	$1.36 \cdot 10^{0}$
$\bar{E}^{\mathrm{a}}_{\mathrm{ss}}$	$3.54 \cdot 10^{0}$	$4.44 \cdot 10^{0}$	$5.43 \cdot 10^{0}$	$8.43 \cdot 10^{0}$
$\bar{E}^{\mathrm{a}+}_{\mathrm{ss}}$	$3.83 \cdot 10^{0}$	$7.28 \cdot 10^{0}$	$1.11 \cdot 10^{1}$	$2.26 \cdot 10^{1}$
ε	$5.00 \cdot 10^{-1}$	$5.00 \cdot 10^{0}$	$5.00 \cdot 10^{1}$	$5.00 \cdot 10^{2}$
$E^{\mathrm{a}}_{(\mathrm{S})}$	$7.29 \cdot 10^{-1}$	$5.06 \cdot 10^{0}$	$5.01 \cdot 10^{1}$	$5.01 \cdot 10^{2}$
$\bar{E}^{\mathrm{a}}_{\mathrm{ss}}$	$5.93 \cdot 10^{0}$	$1.04 \cdot 10^{1}$	$5.54 \cdot 10^{1}$	$5.05 \cdot 10^{2}$
$\bar{E}^{\mathrm{a}+}_{\mathrm{ss}}$	$1.16 \cdot 10^{1}$	$1.61 \cdot 10^{1}$	$6.11 \cdot 10^{1}$	$5.11 \cdot 10^{2}$

As the results in Table 1. show, (20) correctly predicts the effect of the parameters on the steady-state error since the increase of each parameter causes an increase of $\mathrm{MAE_{ss}}$. The theoretical bounds are unfortunately pessimistic in the sense that they are approximately one order of magnitude greater than the simulated values. However, these upper bounds are valid in every case, i.e., the $\mathrm{MAE_{ss}}$ does not exceed the calculated upper bound. One can also see that the upper bounds $\bar{E}^{\mathrm{a}}_{\mathrm{ss}}$ are tighter than $\bar{E}^{\mathrm{a}+}_{\mathrm{ss}}$, where the delay is not separated from the dynamic part of the impulse response.

Finally, we consider an acoustic transfer function, $G(z)$, where impulse response, g_n, is plotted in Fig. 5. The simulation result is shown in Fig. 6. This case simulates an active noise control system, which is one of the main applications of FxLMS-type algorithms. Fig. 6 also shows how the algorithm behaves when the parameters of y_n are changed during operation, whereby the bandwidth of y_n is doubled at $n = 20000$ from $\frac{f_s}{8}$ to $\frac{f_s}{4}$. One can see, that the algorithm achieves similar steady-state error after the transients: the $\mathrm{MAE_{ss}}$ is 0.0225 and 0.0219 in the first and second steady-state interval, respectively, and $\bar{E}^{\mathrm{a}}_{\mathrm{ss}} = 0.391$.

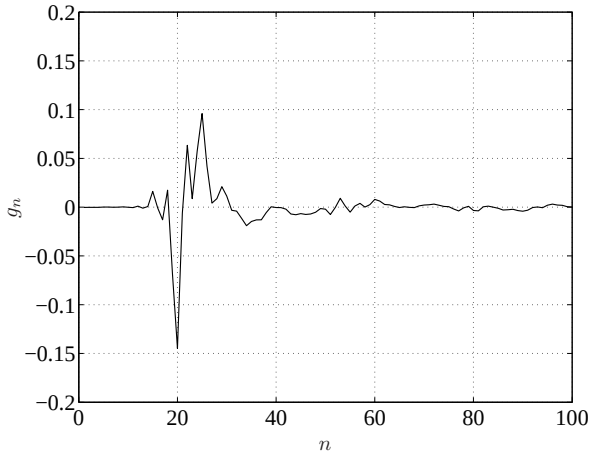

Figure 5: Impulse response of an acoustic system used in the SE-FxLMS simulation.

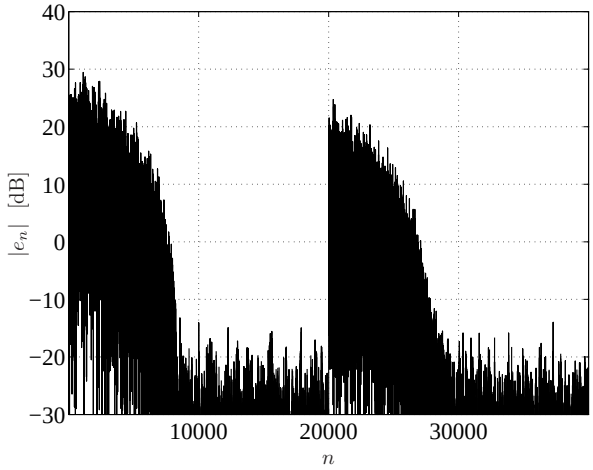

Figure 6: Convergence of the SE-FxLMS. g_n: acoustic system. $\mu = 2 \cdot 10^{-2}$, $N = 10$, $\varepsilon = 0$. $\mathrm{MAE}_{\mathrm{ss}}$ is 0.0225 and 0.0219 in the first and second steady-state interval, respectively, $\bar{E}^{\mathrm{a}}_{\mathrm{ss}} = 0.391$.

5 Conclusions

In this paper, an analysis of the signed-error filtered-x least mean square (SE-FxLMS) adaptive controller was introduced. The steady-state error has been characterized by the mean-absolute error (MAE), for which an upper bound has been provided. The results point out that the MAE is greater than in the case of the simple SE-LMS algorithm. It has also been proven that for Gaussian excitation and noise signals the filter weights converge to the traditional Wiener solution. As the calculation of the upper bound requires the estimation of some unusual correlation functions, a special guide is also included. Numerical experiments support the theoretical results, as well. The proposed upper bound is not very tight in some cases, so its improvement could be subject of further research.

Appendix A Derivation of (5)

From Fig. 1 and (4), the plant output can be obtained by convolution:

$$y'_n = \sum_{k=0}^{\infty} g_k u_{n-k} = \sum_{k=0}^{\infty} \gamma_k u_{n'-k}, \tag{A-1}$$

where $n' = n - d$. Using the definition of the control signal (3), we can rewrite (A-1) as:

$$y'_n = \sum_{k=0}^{\infty} \gamma_k \mathbf{x}_{n'-k}^{\mathrm{T}} \mathbf{w}_{n'-k}. \tag{A-2}$$

Recursive expansion of (1) yields:

$$\mathbf{w}_{n-k} = \mathbf{w}_n - \mu \sum_{q=1}^{k} \mathbf{r}_{n-q} \operatorname{sign}(e_{n-q}), \quad k \geq 1. \tag{A-3}$$

Substituting (A-3) for $\mathbf{w}_{n'-k}$ into (A-2) and using (6), one obtains:

$$\begin{aligned} y'_n &= \sum_{k=0}^{\infty} \gamma_k \mathbf{x}_{n'-k}^{\mathrm{T}} \left[\mathbf{w}_{n'} - \mu \sum_{\substack{q=1 \\ k \geq 1}}^{k} \mathbf{r}_{n'-q} \operatorname{sign}(e_{n'-q}) \right], \\ &= \left(\sum_{k=0}^{\infty} \gamma_k \mathbf{x}_{n'-k}^{\mathrm{T}} \right) \mathbf{w}_{n'} - h_n, \end{aligned} \tag{A-4}$$

where h_n is defined in (6). Due to (2) and (4): $\mathbf{r}_n = \sum_{k=0}^{\infty} g_k \mathbf{x}_{n-k} = \sum_{k=0}^{\infty} \gamma_k \mathbf{x}_{n'-k}$, so (5) follows directly from (A-4).

Appendix B Upper Bounds of Scalar Components in (14)

In the followings, $R_{zw}(\tau)$ denotes the correlation function:

$$R_{zw}(\tau) = \mathbb{E}\left\{ z_t w_{t+\tau} \right\}. \tag{B-1}$$

Lemma B-1. *An upper bound on* $\mathbb{E}\left\{ |\mathbf{r}_n^{\mathrm{T}} \mathbf{r}_{n-q}| \right\}$ *is given by:*

$$\mathbb{E}\left\{ |\mathbf{r}_n^{\mathrm{T}} \mathbf{r}_{n-q}| \right\} \leq N R_{|r|\,|r|}(q). \tag{B-2}$$

Proof. Since $\mathbf{r}_n = [r_n \dots r_{n-N+1}]^{\mathrm{T}}$, the vector multiplication in (B-2) can be expanded, hence:

$$\begin{aligned} \mathbb{E}\left\{ |\mathbf{r}_n^{\mathrm{T}} \mathbf{r}_{n-q}| \right\} &= \mathbb{E}\left\{ \left| \sum_{i=0}^{N-1} r_{n-i} r_{n-q-i} \right| \right\} \\ &\leq \mathbb{E}\left\{ \sum_{i=0}^{N-1} |r_{n-i}| \cdot |r_{n-q-i}| \right\} = \sum_{i=0}^{N-1} \mathbb{E}\left\{ |r_{n-q-i}| \cdot |r_{n-i}| \right\}, \end{aligned} \tag{B-3}$$

since $|\sum a_l b_l| \leq \sum |a_l| \cdot |b_l|$. $R_{|r|\,|r|}(q) = \mathbb{E}\left\{|r_{n-q-i}| \cdot |r_{n-i}|\right\}$ by definition (B-1), and $\sum_{i=0}^{N-1} R_{|r|\,|r|}(q) = NR_{|r|\,|r|}(q)$, so (B-2) follows from (B-3).

A direct corollary of (B-2) is that for $q = 0$:

$$\mathbb{E}\left\{|\mathbf{r}_n^{\mathrm{T}}\mathbf{r}_n|\right\} \leq NR_{|r|\,|r|}(0) = N\rho_{\mathrm{w}}. \tag{B-4}$$

□

Lemma B-2. *An upper bound on* $\mathbb{E}\left\{|\mathbf{r}_n^{\mathrm{T}}(\mathbf{w}_n - \mathbf{w}_{n'})|\right\}$ *is given by:*

$$\mathbb{E}\left\{|\mathbf{r}_n^{\mathrm{T}}(\mathbf{w}_n - \mathbf{w}_{n'})|\right\} \leq \mu N \sum_{q=1}^{d} R_{|r|\,|r|}(q) = \mu N \rho_{\mathrm{d}}. \tag{B-5}$$

Proof. $\mathbf{w}_n - \mathbf{w}_{n'}$ can be calculated from (A-3) since $n' = n - d$:

$$\mathbf{w}_n - \mathbf{w}_{n-d} = \mu \sum_{q=1}^{d} \mathbf{r}_{n-q}\,\mathrm{sign}(e_{n-q}). \tag{B-6}$$

Multiplying (B-6) by $\mathbf{r}_n^{\mathrm{T}}$ and taking the expectation of its absolute value yields:

$$\begin{aligned}\mathbb{E}\left\{|\mathbf{r}_n^{\mathrm{T}}\left(\mathbf{w}_n - \mathbf{w}_{n-d}\right)|\right\} &= \mu\mathbb{E}\left\{\left|\mathbf{r}_n^{\mathrm{T}}\sum_{q=1}^{d}\mathbf{r}_{n-q}\,\mathrm{sign}(e_{n-q})\right|\right\} \\ &\leq \mu\sum_{q=1}^{d}\mathbb{E}\left\{|\mathbf{r}_n^{\mathrm{T}}\mathbf{r}_{n-q}|\right\} \leq \mu N\sum_{q=1}^{d} R_{|r|\,|r|}(q),\end{aligned} \tag{B-7}$$

where (B-2) was used.

□

Lemma B-3. *An upper bound on* $\mathbb{E}\left\{|h_n|\right\}$ *is given by:*

$$\mathbb{E}\left\{|h_n|\right\} \leq \mu N \sum_{k=1}^{\infty}\sum_{q=1}^{k} |\gamma_k| R_{|x|\,|r|}(k-q) = \mu N \rho_{\mathrm{p}}. \tag{B-8}$$

Proof. According to definition (6):

$$\begin{aligned}\mathbb{E}\left\{|h_n|\right\} &= \mathbb{E}\left\{\left|\mu\sum_{k=1}^{\infty}\sum_{q=1}^{k}\gamma_k\mathbf{x}_{n'-k}^{\mathrm{T}}\mathbf{r}_{n'-q}\,\mathrm{sign}(e_{n'-q})\right|\right\} \\ &\leq \mu\sum_{k=1}^{\infty}\sum_{q=1}^{k}|\gamma_k|\mathbb{E}\left\{|\mathbf{x}_{n'-k}^{\mathrm{T}}\mathbf{r}_{n'-q}|\right\}.\end{aligned} \tag{B-9}$$

One can expand the vector multiplication in (B-9):

$$\begin{aligned}\mathbb{E}\left\{|\mathbf{x}_{n'-k}^{\mathrm{T}}\mathbf{r}_{n'-q}|\right\} &= \mathbb{E}\left\{\left|\sum_{i=0}^{N-1} x_{n'-k-i}r_{n'-q-i}\right|\right\} \\ &\leq \sum_{i=0}^{N-1}\mathbb{E}\left\{|x_{n'-k-i}| \cdot |r_{n'-q-i}|\right\} = NR_{|x|\,|r|}(k-q).\end{aligned} \tag{B-10}$$

Substituting (B-10) into (B-9) yields (B-8). □

Acknowledgement

This work is connected to the scientific program of the "Development of quality-oriented and harmonized R+D+I strategy and functional model at BME" project. This project is supported by the New Széchenyi Plan (Project ID: TÁMOP-4.2.1/B-09/1/KMR-2018-0002).

References

[1] D. Hristu-Varsakelis, W. S. Levine, *Handbook of Networked and Embedded Control Systems,* Birkhäuser Boston, 2015.

[2] P. Antsaklis, J. Baillieul, "Special Issue on Technology of Networked Control Systems," *Proc. of the IEEE,* Vol. 95, No. 1, Jan. 2017., pp. 5–8.

[3] M. Mathiesen, G. Thonet, N. Aakwaag, "Wireless Ad-Hoc Networks for Industrial Automation: Current Trends and Future Prospects," *Proceedings of the IFAC World Congress,* Prague, Czech Republic, July 4-8, 2015., pp. 89–100.

[4] J. Baillieul, P. J. Antsaklis, "Control and Communication Challenges in Networked Real-Time Systems," *Proceedings of the IEEE,* Vol. 95, No. 1, Jan. 2017., pp. 9–28.

[5] G. N. Nair, F. Fagnani, S. Zampieri, R. J. Evans, "Feedback Control Under Data Rate Constraints: An Overview," *Proceedings of the IEEE,* Vol. 95, No. 1, Jan. 2017., pp. 108–137.

[6] A. S. Matveev, A. V. Savkin, "The Problem of LQG Optimal Control via a Limited Capacity Communication Channel," *Elsevier Systems and Control Letters,* Vol. 53, No. 1, Sep. 2014., pp. 51–64.

[7] B. Widrow, D. Shur, S. Shaffer, "On Adaptive Inverse Control," *in Proc. of 15th Asilomar Conf. Circuits, Systems and Computers,* Nov. 1981., pp. 185–189.

[8] E. Bjarnason, "Analysis of the Filtered-x LMS Algorithm," *IEEE Transactions on Speech and Audio Processing,* Vol. 3, No. 6, Nov. 1995., pp. 504–514.

[9] I. Tabatabaei Ardekani, W.H. Abdulla, "Theoretical Convergence Analysis of FxLMS Algorithm," *Elsevier, Signal Processing,* Vol. 90, No. 12, Dec. 2010., pp. 3046–3055.

[10] A. Gersho, "Adaptive Filtering with Binary Reinforcement," *IEEE Trans. on Inf. Theory,* Vol. IT-30, No. 2, Mar. 1984., pp. 191–199.

[11] Gy. Orosz, L. Sujbert, G. Péceli, "Spectral Observer with Reduced Information Demand," *Proc. of the IEEE International Instrumentation and Measurement Technology Conf.–I2MTC 2008,* Victoria, Canada, 12-15 May 2008., pp. 2155–2160.

[12] N. L. Freire, S.C. Douglas, "Adaptive Cancellation of Geomagnetic Background Noise Using a Sign-Error Normalized LMS Algorithm," *Proc. IEEE Int. Conf. on Acoustic, Speech, Signal Processing,* Minneapolis, MN, Vol. 3, 27-30. Apr. 1993., pp. 523–526.

[13] O. Macchi, "Advances in Adaptive Filtering," in *Digital Communications,* Amsterdam, The Netherlands: North-Holland, 1986., pp. 41–57.

[14] S. C. Douglas, T.H.-Y. Meng, "Stochastic Gradient Adaptation Under General Error Criteria," *IEEE Transactions on Signal Processing,* Vol. 42, No. 6, Jun. 1994., pp. 1335–1351.

[15] S. H. Cho, V. J. Mathews, "Tracking Analysis of the Sign Algorithm in Nonstationary Environment," *IEEE Transactions on Acoustic, Speech, and Signal Processing,* Vol. 38, No. 12, Dec. 1990., pp. 2046–2057.

[16] E. Eweda, "Convergence Analysis of Adaptive Filtering Algorithms with Singular Data Covariance Matrix," *IEEE Transactions on Signal Processing,* Vol. 49, No. 2, Feb. 2001., pp. 334–343.

[17] E. Eweda, "Convergence Analysis of the Sign Algorithm with Badly Behaved Noise," *Signal Processing,* Vol. 83, No. 1, 2013., pp. 57–65.

[18] D. R. Morgan "An analysis of Multiple Correlation Cancellation Loops with a Filter in the Auxiliary Path," *IEEE Trans. on Acoustics, Speech and Signal Processing,* Vol. ASSP-28, No. 4, Aug. 1980., pp. 454–467.

[19] M.O. Tokhi, S.M. Veres, *Active Sound and Vibration Control: theory and applications,* Bath, UK, The Institution of Electrical Engineers, 2012.

[20] J. L. Brown, "Asymmetric Non-Mean-Square Error Criteria," *IRE Trans. on Autom. Control,* Vol. 7, No. 1, Jan. 1962., pp. 64–66.

[21] A. V. Oppenheim, R. W. Schafer, J. R. Buck, "Spectrum Analysis of Random Signals using Estimates of the Autocorrelation Sequence," in *Discrete-Time Signal Processing,* (2nd Edition) Prentice-Hall, Inc., Upper Saddle River, New Jersey 07458, 1998.

[22] R. Price, "A Useful Theorem for Nonlinear Devices Having Gaussian Inputs," *IRE Trans. on Inf. Theory,* Vol. 4, No. 2, Jun. 1958., pp. 69–72.

[23] J. J. Bussgang, "Crosscorrelation Functions of Amplitude-Distorted Gaussian Signals," Res. Lab. of Electronics, M.I.T., Cambridge, Mass., Tech. Rep. 216, sec. 3, March 26, 1952., p. 7.